HELDA
HELSINGIN YLIOPISTO
HELSINGFORS UNIVERSITET
UNIVERSITY OF HELSINKI

UNIVERSITY OF HELSINKI

https://helda.helsinki.fi

Particle growth with photochemical age from new particle formation to haze in the winter of Beijing, China

Chu, Biwu

2021-01-20

Chu , B , Dada , L , Liu , Y , Yao , L , Wang , Y , Du , W , Cai , J , Dällenbach , K R , Chen , X , Simonen , P , Zhou , Y , Deng , C , Fu , Y , Yin , R , Li , H , He , X , Feng , Z , Yan , C , Kangasluoma , J , Bianchi , F , Jiang , J , Kujansuu , J , Kerminen , V-M , Petäjä , T , He , H & Kulmala , M 2021 , ' Particle growth with photochemical age from new particle formation to haze in the winter of Beijing, China ' , The Science of the Total Environment , vol. 753 , 142207 . https://doi.org/10.1016/j.scitotenv.2020.142207

http://hdl.handle.net/10138/348035
https://doi.org/10.1016/j.scitotenv.2020.142207

cc_by_nc_nd
acceptedVersion

Downloaded from Helda, University of Helsinki institutional repository.

This is an electronic reprint of the original article.

This reprint may differ from the original in pagination and typographic detail.

Please cite the original version.

Particle growth with photochemical age from new particle formation to haze in the winter of Beijing, China

Biwu Chu[1, 2, 3, 4,], Lubna Dada[2], Yongchun Liu[1,*], Lei Yao[2], Yonghong Wang[2], Wei Du[2], Jing Cai[2], Kaspar Dällenbach[2], Xuemeng Chen[2], Pauli Simonen[5], Ying Zhou[1], Chenjuan Deng[6], Yueyun Fu[6], Rujing Yin[6], Haiyan Li[2], Xu-Cheng He[2], Zeming Feng[1], Chao Yan[1, 2], Juha Kangasluoma[1, 2], Federico Bianchi[2], Jingkun Jiang[6], Joni Kujansuu[1, 2], Veli-Matti Kerminen[2], Tuukka Petäjä[1, 2, 7], Hong He[3, 4], Markku Kulmala[1, 2, 7]*

[1]Aerosol and Haze Laboratory, Beijing Advanced Innovation Center for Soft Matter Science and Engineering, Beijing University of Chemical Technology, Beijing, China

[2]Institute for Atmospheric and Earth System Research / Physics, Faculty of Science, University of Helsinki, Finland

[3]Center for Excellence in Regional Atmospheric Environment, Institute of Urban Environment, Chinese Academy of Sciences, Xiamen 361021, China

[4]State Key Joint Laboratory of Environment Simulation and Pollution Control, Research Center for Eco-Environmental Sciences, Chinese Academy of Sciences, Beijing 100085, China

[5]Aerosol Physics Laboratory, Physics Unit, Faculty of Engineering and Natural Sciences, Tampere University, Tampere, Finland

[6]State Key Joint Laboratory of Environment Simulation and Pollution Control, School of Environment, Tsinghua University, Beijing 100084, China

[7]Joint International Research Laboratory of Atmospheric and Earth System Sciences, School of Atmospheric Sciences, Nanjing University, Nanjing 210023, China

TOC:

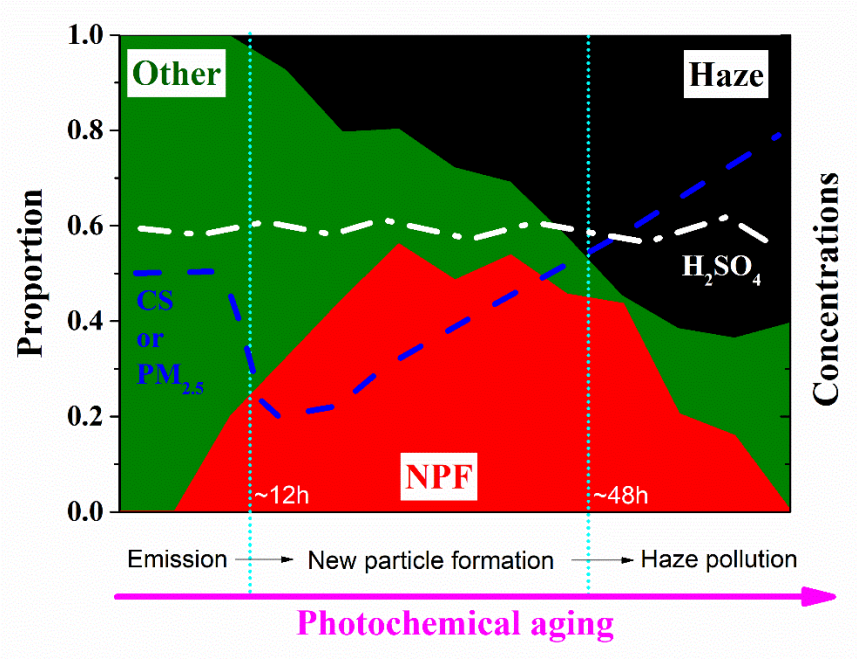

HIGH LIGHTS

The evolution of pollution episodes as a function of photochemical age was studied.

Persistent nucleation with photochemical age ranging from 12-48 h was observed.

CS and $PM_{2.5}$ increased faster with photochemical age on NPF days than other days.

Keywords

photochemical aging; new particle formation; haze; pollution evolution; condensation sink

ABSTRACT.

Secondary aerosol formation in the aging process of primary emission is the main reason for haze pollution in eastern China. Pollution evolution with photochemical age was studied for the first time at a comprehensive field observation station during winter in Beijing. The photochemical age was used as an estimate of the timescale attributed to the aging process and was estimated from the ratio of toluene to benzene in this study. A low photochemical age indicates a fresh emission. The photochemical age of air masses during new particle formation (NPF) days was lower than that on haze days. In general, the strongest NPF events, along with a peak of the formation rate of 1.5 nm ($J_{1.5}$) and 3 nm particles (J_3), were observed when the photochemical age was between 12 and 24 h while rarely took place with photochemical ages less than 12 h. When photochemical age was larger than 48 h, haze occurred and NPF was suppressed. The sources and sinks of nanoparticles had distinct relation with the photochemical age. Our results show that the condensation sink (CS) showed a valley with photochemical ages ranging from 12 to 24 h, while H_2SO_4 concentration showed no obvious trend with the photochemical age. The high concentrations of precursor vapours within an air mass lead to persistent nucleation with photochemical age ranging from 12-48 h in winter. Coincidently, the fast increase of $PM_{2.5}$ mass was also observed during this range of photochemical age. Noteworthy, CS increased with the photochemical age on NPF days only, which is the likely reason for the observation that the $PM_{2.5}$ mass increased faster with photochemical age on NPF days compared with other days. The evolution of particles with the photochemical age provides new insights into understanding how particles originating from NPF transform to haze pollution.

1 Introduction

Atmospheric aerosol particles, originating from both primary emissions and atmospheric oxidation followed by gas-to-particle conversion, have adverse effects on human health and visibility (Kaiser, 2005; Lelieveld et al., 2015; Wang et al., 2015b), and affect the climate (IPCC, 2013). In an urban environment,

secondary atmospheric processes were argued to be the main source of aerosol particles in terms of their number (Kulmala et al., 2016) and mass (Sun et al., 2016). Such secondary processes include the initial new particle formation (NPF) and condensation of gas phase compounds to aerosol surfaces, which results in the growth of the particle size (Kulmala et al., 2014).

In China, the rapid economic development and urbanization have led to high emissions of pollutants from coal combustion, motor vehicle exhaust and industrial activities, which has resulted in highly complex air pollution. High concentrations of trace gases, such as SO_2, NO_x, NH_3 and VOCs (Liu et al., 2013; Wang et al., 2015a; Ye et al., 2011; Zou et al., 2015), have caused high concentrations of secondary inorganic and organic species in fine particles ($PM_{2.5}$) during haze formation (Huang et al., 2012; Yang et al., 2011; Zhao et al., 2013). However, the frequency of NPF events in high aerosol-loading environments were higher than those in low aerosol-loading environments in China(Peng et al., 2014). Compared with rural or urban sites in western countries, the observed particle formation rates were one to two orders of magnitude higher and the particle growth rates (GRs) were also somewhat higher for NPF in China (Chu et al., 2019; Shen et al., 2016; Yao et al., 2018). The extent by which the high concentrations of pollutants or the highly complex cocktail of air pollution influences NPF remains highly uncertain (Chu et al., 2019; Kulmala, 2015; Kulmala et al., 2017). Meanwhile, the contribution of NPF to haze formation is still controversial. With high concentrations of condensable vapours, newly-formed particles have the potential to grow quickly, which results in an increase of PM volume or mass concentrations. The survival of growing particles to larger sizes could then directly affect air quality, visibility and climate(Chu et al., 2019). Guo et al. (2014) reported NPF followed by a continuous growth and appearance of haze pollution in Beijing and proposed that NPF probably led to haze formation. The controversy about the contribution of NPF to haze requires analysing the connections between these two phenomena using suitable parameters.

NPF and haze are dominated by secondary processes in terms of the particle number and mass concentration (Kulmala et al., 2016; Sun et al., 2016). Oxidation of gaseous precursors is usually needed for the gas-to-particle conversion in both NPF and haze formation, in which photooxidation plays an important role. The status of the oxidation process will be dependent on both the concentrations of oxidants in the atmosphere and the photochemical age of the air mass, which is the length of the aging process: a low photochemical age indicates fresh emissions while a high photochemical age indicates aged air mass (Parrish et al., 1992). Particle formation, particle mass growth, visibility decrease and many other processes are expected to occur during different aging periods of the pollutants after their emission, since the limiting factors for these processes are different. However, according to our knowledge, there is no study that investigates NPF and haze evolution with photochemical age. During atmospheric observations, the air mass is constantly changing, which makes it difficult to study chemical transformation in isolation from the effect of air mass transportation in the pollution evolution. Analysing pollution evolution with photochemical age may provide insights into how gaseous pollutants and particles chemically transform with an average emission during different transportation conditions.

A continuous comprehensive atmospheric field observation site was established in urban Beijing in 2018 and has been operating since then (Lu et al., 2019; Zhou et al., 2020). In this study, we investigate the photochemical age and related processes during the winter 2018 in Beijing. We investigated changes in many key factors affecting both NPF and haze, such as particle number and mass concentration, condensation sink (CS, which describes the condensing vapor sink caused by the particle population) and sulfuric acid (H_2SO_4) concentration, as a function of the photochemical age of air, aiming to draw a general picture on the evolution of pollution episodes in winter in Beijing. Based on this general picture, we connect photochemical aging to major atmospheric phenomena, such as NPF and haze formation as well as their intensity. We also investigate the relationship between NPF and haze formation.

2 Research methods

2.1 Comprehensive measurement station in Beijing

The results presented in this study are collected at a comprehensive measurement station in urban Beijing (N 33.94°, E 116.30°) between 23rd of January and 31st March 2018. The observation station is located on the western campus of Beijing University of Chemical Technology (BUCT), which is 400 m to the west of the West Third Ring Road and surrounded by residential and commercial areas (Lu et al., 2019; Zhou et al., 2020). Particle number concentration and size distribution were monitored with a suite of instruments, including a Particle Size Magnifier (PSM) to measure small particles in the range of 1.5 – 2.5 nm (Vanhanen et al., 2011), a diethylene glycol (DEG) SMPS to measure 1.5 – 6 nm particles (Cai et al., 2017; Jiang et al., 2011), a Particle Size Distribution (PSD) to detect particles from 3 nm to 10 μm (Liu et al., 2016), and a neutral cluster and air ion spectrometer (NAIS) to monitor the 0.8 – 20 nm ions and 2 – 20 nm particles (Mirme and Mirme, 2013). More detailed information for particle size distribution measurements and calibrations can be found in section 1 of the supporting Information (SI). These data were mainly used to calculate the CS, particle formation and growth rates (Kulmala et al., 2012), and to identify NPF events, which are characterized by the burst of nucleation mode (sub– 25 nm) particles and subsequent growth and are classified with the method introduced by Dal Maso et al. (2005) The detail information about the calculation methods and the criteria for identifying an NPF event can be found in sections 2, 3 and 4 of the SI.

Air quality was monitored with various instruments, including gas analyzers (model 42i-TL, 43i-TLE, 48i-TLE, and 49i, Thermo Scientific) to measure mixing ratios of trace gases (NO_x, SO_2, CO, and O_3), and an online single photo ionization time-of-flight mass spectrometer (SPI-ToF-MS 3000R, Hexin Mass Spectrometry) (Gao et al., 2013) to measure VOCs, which cannot distinguish isomers but only identify

VOC species with unit mass resolution. Meteorological parameters (temperature, relative humidity, ultraviolet radiation (UVB), pressure, wind speed and direction) and visibility were measured by an automatic weather station (QML201C and PWD22, Vaisala Inc.). $PM_{2.5}$ mass concentration used in this study was the average value of the four surrounding national observation stations operated by the China National Environmental Monitoring Center (Website: http://www.cnemc.cn), while the composition of $PM_{2.5}$ was measured with an time-of-flight Aerosol Chemical Speciation Monitor (ToF-ACSM, Aerodyne Inc.) (Frohlich et al., 2013). These data were used to identify haze events, which were mainly characterized as the visibility less than 10 km and the relative humidity less than 80% (see more detail in section 4 of the SI), and also to analyse the pollution characteristics. Besides, the sulfuric acid (H_2SO_4) and highly oxygenated organic molecules (HOM) in the gas phase were measured by a chemical ionization long time-of-flight mass spectrometer (LToF-CIMS, Aerodyne Research, Inc.) equipped with a nitrate chemical ionization source (see more detail in section 5 of the SI).

2.2 Photochemical age of air mass

Hydroxyl radical (OH) is the most important oxidant in the atmosphere. Assuming that two different volatile organic compounds (VOCs) are simultaneously introduced into an air parcel and react with OH radical at different rates following pseudo-first-order kinetics and neglecting the influences of dilution, the ratio of the concentrations of the two VOCs was used to estimate the photochemical aging of the emission, i.e. the so-called the photochemical age in this study (Parrish et al., 1992). Alkanes in the atmosphere are primarily removed by oxidation in bimolecular reactions with OH, and the reaction can be assumed pseudo-first-order because the OH concentration is not significantly affected by the reaction with the alkane but is determined by a steady state governed by much faster production and removal reactions [22]. Similar assumptions can also be applied to some aromatics, such as toluene and benzene. Since toluene reacts faster with OH radical than benzene, the ratio of toluene to benzene will decrease due

to aging. Toluene and benzene have widespread sources such as traffic, industry and solvent use (Gao et al., 2018 and references therein). In Beijing, traffic might be the most important contributor to these VOC emissions, in which toluene and benzene are emitted simultaneously (Gao et al., 2018). Since there is abundance of toluene and benzene in the atmosphere and isomers have no significant influence on their concentration measurement, the ratio between toluene and benzene is used to estimate the photochemical age in this study. They are selected as the representative VOCs of the local emission source at our observation site that is surrounded by heavy traffic. NPF and haze take usually place in a regional scale. In North China Plain, traffic was estimated to be one of the main emission sources of air pollution(Liu et al., 2013). Besides traffic, coal burning is another important emission source (Sun et al., 2016) which also emits toluene and benzene (Gao et al., 2018 and references therein). Therefore, toluene and benzene could be used as the representative VOCs of the regional emission sources.

Generally, the photochemical age t_{a} was derived from the following equation in this study:

$$t_{\mathrm{a}} = \frac{LN\left[\frac{C_{\mathrm{toluene}}}{C_{\mathrm{benzene}}}(t_0)\right] - LN\left[\frac{C_{\mathrm{toluene}}}{C_{\mathrm{benzene}}}(t)\right]}{(k_{\mathrm{toluene+OH}} - k_{\mathrm{benzene+OH}}) \times \mathrm{OH}} \qquad (1)$$

where $\frac{C_{\mathrm{toluene}}}{C_{\mathrm{benzene}}}(t_0)$ and $\frac{C_{\mathrm{toluene}}}{C_{\mathrm{benzene}}}(t)$ are the mole concentration ratios of toluene to benzene at the initial emission time and the observation time, respectively $k_{\mathrm{toluene+OH}}$ and $k_{\mathrm{benzene+OH}}$ are the rate constants for reactions of toluene and benzene with OH radical, respectively. OH concentrations varies a lot ($< 1 \times 10^6$–1.7×10^7 molecules cm^{-3}) in different seasons and under different whether conditions (Lu et al., 2013; Tan et al., 2018; Yang et al., 2017). To be comparable with prior publications (Chu et al., 2016; Liu et al., 2018; Mao et al., 2009), the average OH concentration in the winter of Beijing was assumed to be 1.5×10^6 molecules cm^{-3} in this study. Varied concentrations of OH will speed up or slow down the pollution evolution with time, but will not change the picture of pollution evolution with photochemical age since

using photochemical age actually converts the pollution evolution with time to pollution evolution with OH exposure. In this study, the 99th percentile of observed ratios of toluene to benzene (i.e. 2.11) was assumed to be the mole concentration ratio between toluene and benzene at the initial emission time. This ratio is consistent with the value that can be calculated from the emission ratio (ER) of toluene and benzene in Beijing (Yuan et al., 2012), and it is also close to the slope of the upper "edge" in the scatterplot (Figure S5 in section 6 of the SI). We have to point out that mixing with other air masses (fresher emission, more aged air mass, or air mass with significant different emission sources) during the dilution or transport will influence the photochemical age. A detailed introduction of the calculation method and its uncertainty analysis can be found in section 6 of the SI. Basically, aging two air masses separately and then mixing will result in a little slower aging process compare to mixing two air masses firstly and then aging the mixture for an pollutant-mass-weighted average photochemical age of the two air masses.

3 Results and discussions

3.1 Variation of photochemical age on different pollution events

During the observation period, days were classified into three groups (Figure S3 in section 4 of the SI): NPF days (35 days), haze days (23 days) and other days when no NPF nor haze was observed (10 days). In this study, full 24 hours of data were used in analyzing the haze days as haze events usually lasted for a few days, whereas the data between 7:00 and 17:00 were used in analyzing the NPF days (except that the full 24 hours of data were used in Figure 1) as all the NPF events took place in this time window (Dada et al. 2018, Zhou et al. 2020, and references therein). The diurnal variations of photochemical age of air mass on these three types of days are displayed in Figure 1a. Overall, the photochemical age of the air mass on NPF days was lower (by 22% on average) than that on haze days (the p-value for hypothesis test in statistics is less than 0.05, which means there is a <5% chance that the results could be random), as

shown in Figure S6 in section 6 of the SI. This observation can be attributed to the fact that a few hours of photochemical reactions are able to accumulate enough precursors for NPF to occur, while a longer period of atmospheric aging is needed to accumulate high enough concentration of particle mass for haze. The photochemical age increased by about 9-12 hours during a 4-hour period from 8:00 to 12:00 in the morning of all the three types of days excluding haze days. In other words, the air underwent 2-3 hours photochemical aging each hour during these periods, which may indicate that the actual concentration of OH was about 2-3 times the assumed 1.5×10^{6} molecules cm^{-3}. The increase of photochemical age would also be accelerated in the case of mixing with a more aged air mass at the observation site. However, this was unlikely as there was no particular wind direction or wind speed change in the morning. The photochemical age of the air mass on NPF days was not statistically significantly different from the 'other' days in the daytime (p-value < 0.05), but it was higher in the evening. Fresh local emissions associated with a small photochemical age seem not to favour the occurrence of NPF in the winter of Beijing, as NPF rarely took place when the photochemical age was less than 12 h (Figure 1b). As photochemical age increased, the probability of NPF occurrence increased as well, however, if the photochemical age was too large, NPF was suppressed and haze was likely to take place.

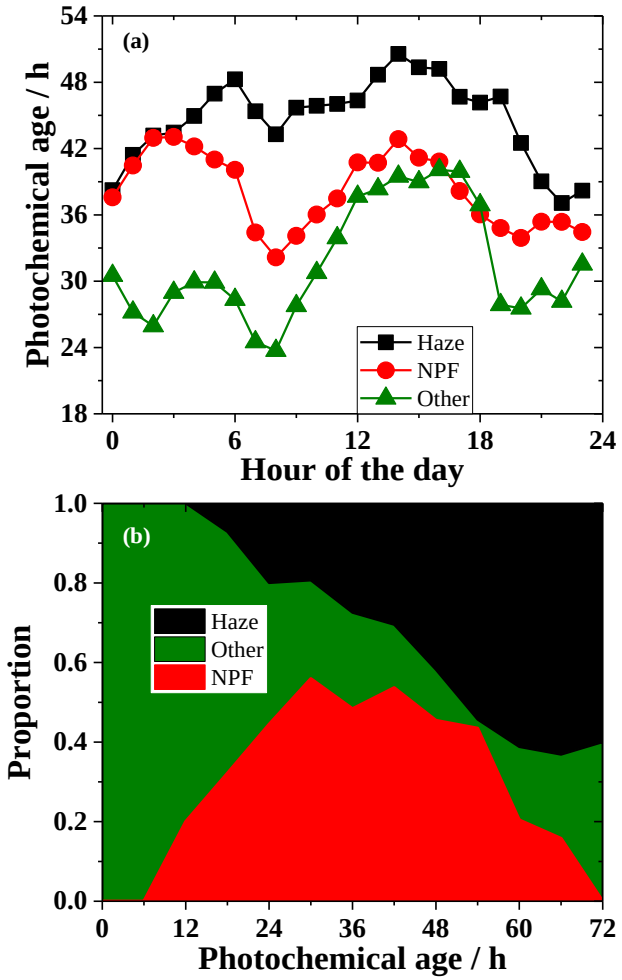

Figure 1: Median diurnal variations of the photochemical age on different groups of days (a) and probability of NPF and haze occurrence as a function of photochemical age (b) during winter Beijing. The full 24 hours of data were used in the analysis for this figure.

3.2 Effects of photochemical age on particle formation and growth

The median values of some pollutant concentrations and NPF parameters in each bin of photochemical age are shown in Figure 2 to display the average case for the evolution of pollution with photochemical age. As indicated by the median aerosol number size distribution in Figure 2a, an obvious formation of sub-10 nm particles was observed when the photochemical age of the air mass ranged between 12 h and 48 h, and the $PM_{2.5}$ mass concentration also showed an obvious growth over this photochemical age range

(Figure 2b). When photochemical age was less than 12 h, i.e. primary emissions dominated the pollution, the frequency of NPF (Figure 1b) and the number concentrations of sub-10 nm particles (Figure 2a) were low, while the $PM_{2.5}$ mass concentration was usually relatively high and resulted in relatively high CS compare to that with photochemical age ranging from 12 h to 24 h (Figure 2b). NPF seemed to be the strongest for a photochemical age ranging from 12 h to 24 h, and became thereafter weaker, which indicates that NPF is favoured by relatively fresh air in Beijing winter. Both $J_{1.5}$ and J_3, which are the growth flux through a certain particle diameter, i.e. 1.5 nm and 3 nm (see more detail in section 3 of the SI), showed a peak and CS showed a valley for the photochemical age ranging from 12 h to 24 h (Figure 2b and c). At photochemical ages larger than 48 h, NPF rarely took place. Meanwhile, the $PM_{2.5}$ mass concentration exceeded 75 μg m^{-3}, which is the secondary air quality standard in China[1], and visibility rapidly dropped to 10 km indicating haze, as shown in Figure 2b.

In Figure 2c, the variations of gas phase HOM and H_2SO_4 concentrations with photochemical age are shown. There was no obvious change in the H_2SO_4 concentrations with photochemical age, while HOM showed a decreasing trend. As shown by previous studies (Lu et al., 2019; Petäjä et al., 2009), the H_2SO_4 concentration is proportional to OH radical and SO_2 concentrations, while being inversely proportional to CS. The stable H_2SO_4 concentrations with photochemical age might be due to a balance of increasing SO_2 concentrations and CS during the accumulation of pollutants, as shown in Figure 2d and b, respectively. H_2SO_4 is a key precursor of nucleation for NPF in megacities when stabilized by strong base molecules such as ammonia or amines [17]. The independence of the H_2SO_4 concentration from the photochemical age indicates that there are abundant H_2SO_4 precursors for NPF to occur over a wide range of photochemical ages or rather that regardless of the photochemical age. H_2SO_4 seems not to be the limiting factor for NPF

[1] GB 3095—2012, http://kjs.mee.gov.cn/hjbhbz/bzwb/dqhjbh/dqhjzlbz/201203/t20120302_224165.shtml, 2019/08/19

to occur. The high concentrations of H_2SO_4 within the air mass with a relatively large photochemical age led to persistent atmospheric nucleation, which can be seen from the fact that $J_{1.5}$ did not drop below 10 cm^{-3} s^{-1} throughout the whole range of photochemical ages in Figure 2c. Although not all newly-formed clusters survive to initiate an NPF event due to their loss to pre-existing particles (high CS), coagulation of clusters and condensation of vapours, such as H_2SO_4 and HOMs, onto aerosol surface will continuously contribute to the particle growth. Similar as H_2SO_4, which was proportional to SO_2 concentrations and inversely proportional to CS (Lu et al., 2019; Petäjä et al., 2009), the HOM concentration is likely to be proportional to the concentrations of its VOC precursors, while being inversely proportional to CS. The decreasing trend of HOM concentration with an increasing photochemical age is likely due to the increased CS and decreased concentrations of some of the high-reactivity VOC precursors, such as toluene in Figure 2d, which could be oxidized to generate HOM (Molteni et al., 2018). A growing number of studies reported that HOMs are key contributors to the particle growth (Bianchi et al., 2019 and references therein), however, their pollution characterization and sources need more dedicated studies especially in urban environments.

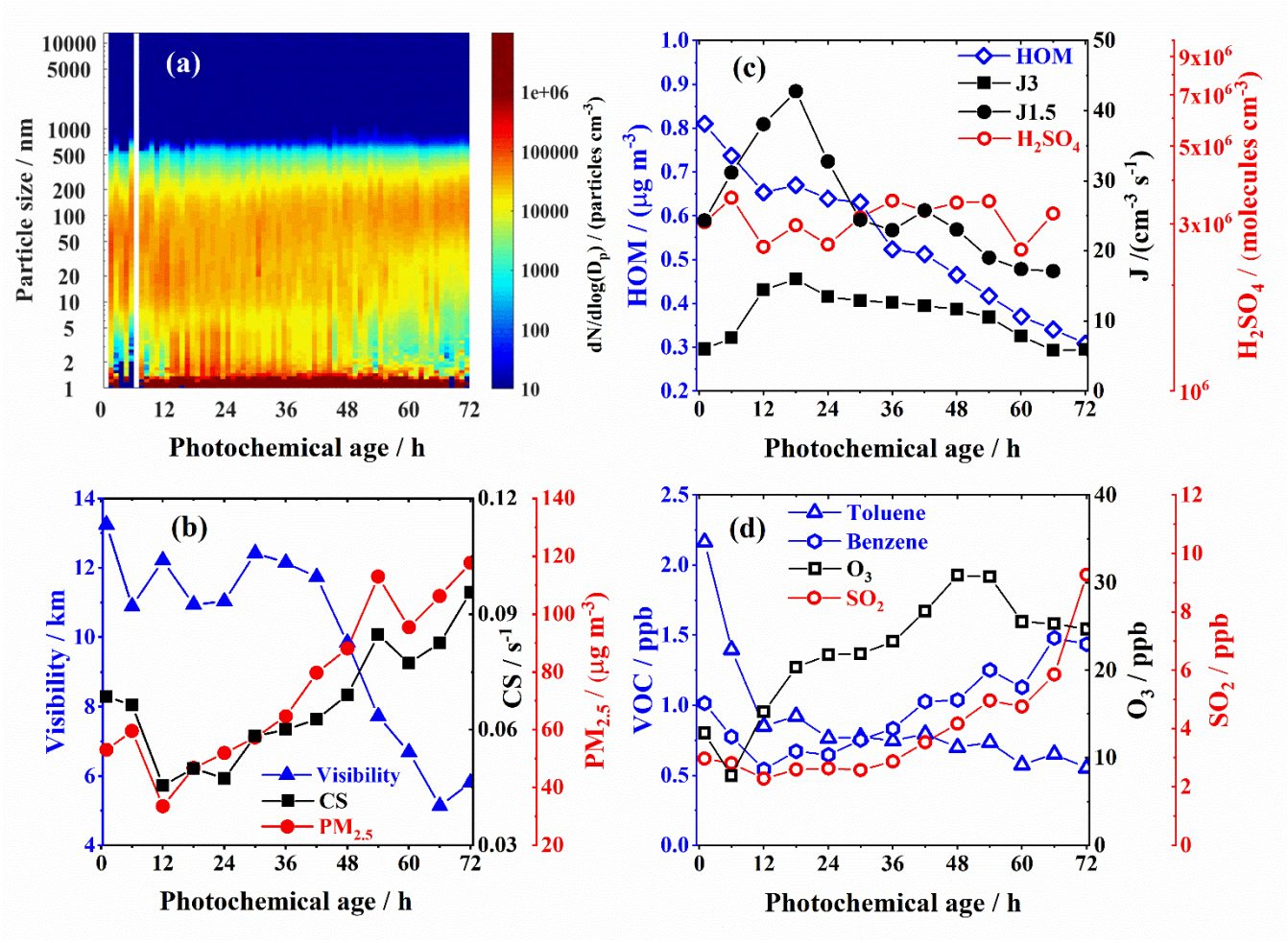

Figure 2: Variation of aerosol size distribution (a), visibility, CS, and $PM_{2.5}$ (c), HOM concentrations, the formation rates of 1.5 nm ($J_{1.5}$) and 3 nm particles (J_3), and H_2SO_4 concentrations (c), and trace gas (toluene, benzene, O_3, and SO_2) concentrations (d) with photochemical age from Equation (1).

Figure 3 shows the number concentrations of nucleation mode (3-25 nm), Aitken mode (25-100 nm) and accumulation mode (100-1000 nm) aerosol particles, CS and $PM_{2.5}$ as a function of photochemical age on different days. Sub-100 nm particle number concentrations showed a decreasing trend with photochemical age on non-NPF days, while no such trend was observed on NPF days (Figure 3a and b). There is an increasing trend of accumulation mode particles with photochemical age on the NPF days but not on the non-NPF days (Figure 3c). These results indicate that NPF contributed not only to the nucleation mode particle number concentration, but also to the Aitken mode and accumulation mode particle number

concentrations. On days with no NPF, CS decreased with the photochemical age, while it increased with the photochemical age on NPF days (Figure 4a). On the other hand, increases of $PM_{2.5}$ mass concentrations were observed on all the three types of days with the development of photochemical age, regardless of whether haze or NPF event occurred or not. In general, $PM_{2.5}$ mass concentrations were lower on NPF days, as shown in Figure 4b and previous studies (Chu et al., 2019 and references therein). The lower $PM_{2.5}$ mass concentrations are expected to be associated with weaker sources of gas pollutants, including the condensing precursors. However, the increase rate of $PM_{2.5}$ mass accumulation with photochemical age on NPF days (0.5 $\mu g\ m^{-3}\ h^{-1}$) turned out to be faster than that on non-NPF days (about 0.2 $\mu g\ m^{-3}\ h^{-1}$), as shown in Figure 4b. With photochemistry activity differences already considered in the photochemical age, this phenomenon might result from the increase of CS with photochemical age on NPF days. Adopting this point of view, we hypothesize that NPF could have an important contribution to the increase of $PM_{2.5}$ mass concentration in the winter of Beijing participating in haze formation.

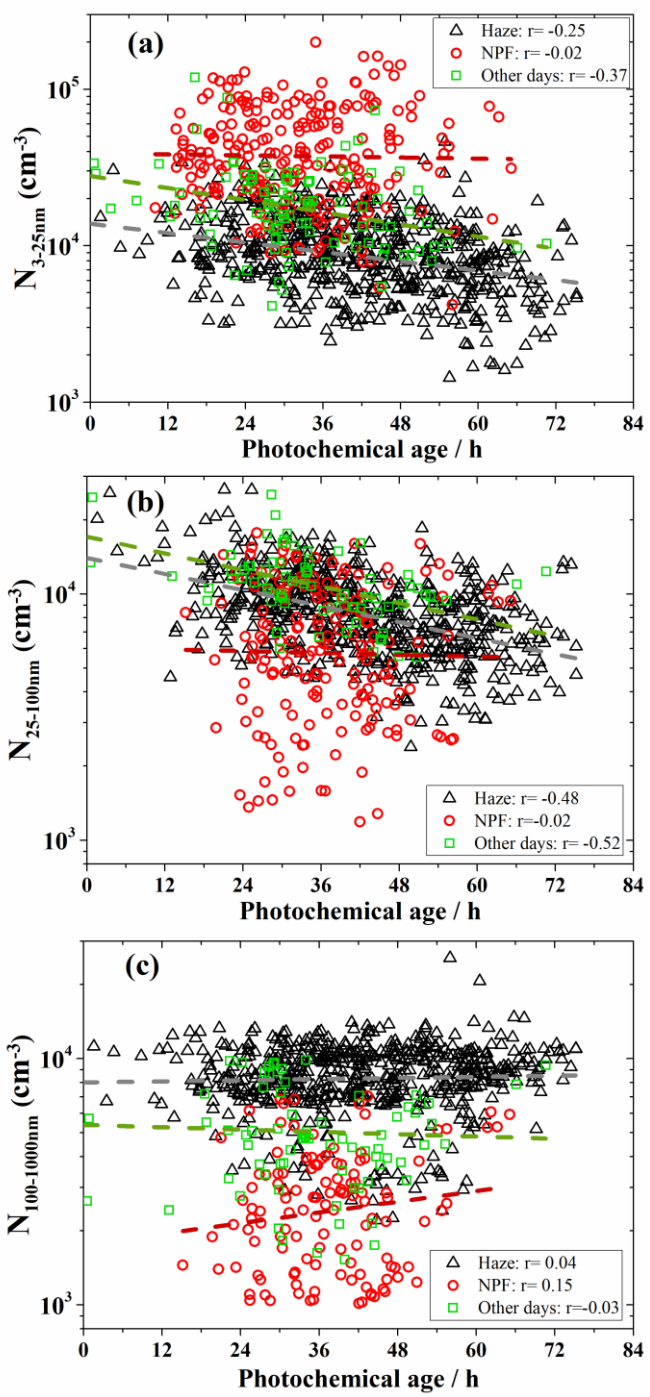

Figure 3: Trends of hourly averages of number concentrations of Nucleation mode (3-25 nm) (a), Aitken mode (25-100 nm) (b) and accumulation mode (100-1000 nm) (c) aerosols with photochemical age in NPF and haze days. The dark grey, dark red and dark green dashed lines in the pictures are the linear fitting of the data points for haze days, NPF days and other days with no haze and no NPF, respectively. Pearson's r is displayed for each fitting.

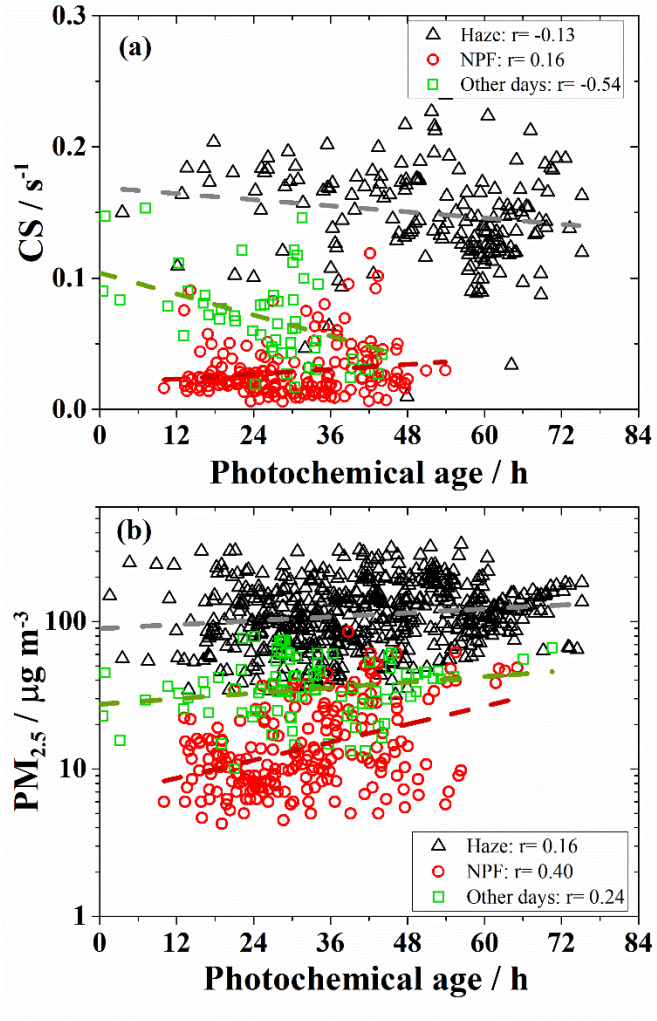

Figure 4: Trends of hourly averages of condensation sinks (a) and $PM_{2.5}$ mass concentrations (b) with photochemical age in NPF and haze days. The dark grey, dark red and dark green dashed lines in the pictures are the linear fitting of the data points for haze days, NPF days and other days with no haze and no NPF, respectively. Pearson's r is displayed for each fitting.

4. Conclusions

We draw a general picture of the evolution of pollution episodes as a function of photochemical age in winter of Beijing based on a comprehensive measurement station for the first time. A few hours of photochemical reactions are able to accumulate enough precursors for NPF to occur, while a longer period of atmospheric aging is needed to accumulate high enough concentration of particle mass for haze. Fresh

local emissions associated with a small photochemical age and haze pollution associated with a large photochemical age do not favour the occurrence of NPF in the winter of Beijing. In an average situation, the frequency of NPF was low when the photochemical age was lower than 12 h, while the strongest nucleation (highest $J_{1.5}$ and J_3) took place with photochemical ages ranging from 12 h to 24 h, and then became weaker as photochemical age increased further. With photochemical age larger than 48 h, haze was always present and NPF disappeared. H_2SO_4 concentration showed no obvious trend with photochemical age due to the balance of increasing SO_2 concentrations and CS with photochemical age in the atmosphere. The high concentrations of precursors in the air mass lead to a persistent nucleation with photochemical age ranging from 12 h to 48 h in the winter of Beijing. Coincidently, the fast increase of $PM_{2.5}$ and CS was also observed during this range of photochemical ages. These results highlighted that nucleation and subsequent growth of nucleated particles, when strong enough, can contribute to CS, $PM_{2.5}$ and even haze.

AUTHOR INFORMATION

Corresponding Author

Biwu Chu (bwchu@rcees.ac.cn) or Yongchun Liu (liuyc@buct.edu.cn)

Author Contributions

BC, YL and MK designed the research. BC, LD, YL, LY, YW, WD, JC, KD, YZ, CD, YF, RY, HL, XCH, ZF, and CY carried out the observation and analyzed the data from different instruments. BC, LD, XC, PS, J., Kangasluoma, FB, JJ, J., Kujansuu, VMK, TP, HH and MK analyzed the observation results. BC prepared the manuscript with contributions from all co-authors.

ACKNOWLEDGMENT

This work was supported by the National Natural Science Foundation of China (41877304, 41877306), Academy of Finland (1251427, 1139656, 296628, 306853, Finnish centre of excellence 1141135), the EC Seventh Framework Program and European Union's Horizon 2020 program (ERC, project no.742206 "ATM-GTP"), and the Youth Innovation Promotion Association, CAS (2018060).

REFERENCES

Bianchi F, Kurtén T, Riva M, Mohr C, Rissanen MP, Roldin P, et al. Highly Oxygenated Molecules (HOM) from Gas-Phase Autoxidation Involving Organic Peroxy Radicals: A Key Contributor to Atmospheric Aerosol. Chemical Reviews 2019.

Cai RL, Chen DR, Hao JM, Jiang JK. A miniature cylindrical differential mobility analyzer for sub-3 nm particle sizing. Journal of Aerosol Science 2017; 106: 111-119.

Chu B, Liu Y, Ma Q, Ma J, He H, Wang G, et al. Distinct potential aerosol masses under different scenarios of transport at a suburban site of Beijing. Journal of Environmental Sciences 2016; 39: 52-61.

Chu BW, Kerminen VM, Bianchi F, Yan C, Petaja T, Kulmala M. Atmospheric new particle formation in China. Atmospheric Chemistry and Physics 2019; 19: 115-138.

Dada L, Chellapermal R, Buenrostro Mazon S, Paasonen P, Lampilahti J, Manninen HE, et al. Refined classification and characterization of atmospheric new-particle formation events using air ions. Atmos. Chem. Phys. 2018; 18: 17883-17893.

Dal Maso M, Kulmala M, Riipinen I, Wagner R, Hussein T, Aalto PP, et al. Formation and growth of fresh atmospheric aerosols: eight years of aerosol size distribution data from SMEAR II, Hyytiala, Finland. Boreal Environment Research 2005; 10: 323-336.

Frohlich R, Cubison MJ, Slowik JG, Bukowiecki N, Prevot ASH, Baltensperger U, et al. The ToF-ACSM: a portable aerosol chemical speciation monitor with TOFMS detection. Atmospheric Measurement Techniques 2013; 6: 3225-3241.

Gao J, Zhang J, Li H, Li L, Xu LH, Zhang YJ, et al. Comparative study of volatile organic compounds in ambient air using observed mixing ratios and initial mixing ratios taking chemical loss into account - A case study in a typical urban area in Beijing. Science of the Total Environment 2018; 628-629: 791-804.

Gao W, Tan GB, Hong Y, Li M, Nian HQ, Guo CJ, et al. Development of portable single photon ionization time-of-flight mass spectrometer combined with membrane inlet. International Journal of Mass Spectrometry 2013; 334: 8-12.

Guo S, Hu M, Zamora ML, Peng JF, Shang DJ, Zheng J, et al. Elucidating severe urban haze formation in China. Proceedings of the National Academy of Sciences of the United States of America 2014; 111: 17373-17378.

Huang C-H, Chen K-S, Wang H-K. Measurements and PCA/APCS Analyses of Volatile Organic Compounds in Kaohsiung Municipal Sewer Systems, Southern Taiwan. Aerosol and Air Quality Research 2012; 12: 1315-1326.

IPCC. Working group I contribution to the IPCC fifth Assessment Report (AR5), climate change 2013: the physical science basis, Geneva, Switzerland. 2013.

Jiang J, Chen M, Kuang C, Attoui M, McMurry PH. Electrical Mobility Spectrometer Using a Diethylene Glycol Condensation Particle Counter for Measurement of Aerosol Size Distributions Down to 1 nm. Aerosol Science and Technology 2011; 45: 510-521.
Kaiser J. How dirty air hurts the heart. Science 2005; 307: 1858-1859.
Kulmala M. China's choking cocktail. Nature 2015; 526: 497-499.
Kulmala M, Kerminen VM, Petaja T, Ding AJ, Wang L. Atmospheric gas-to-particle conversion: why NPF events are observed in megacities? Faraday Discuss 2017; 200: 271-288.
Kulmala M, Luoma K, Virkkula A, Petaja T, Paasonen P, Kerminen VM, et al. On the mode-segregated aerosol particle number concentration load: contributions of primary and secondary particles in Hyytiala and Nanjing. Boreal Environment Research 2016; 21: 319-331.
Kulmala M, Petaja T, Ehn M, Thornton J, Sipila M, Worsnop DR, et al. Chemistry of Atmospheric Nucleation: On the Recent Advances on Precursor Characterization and Atmospheric Cluster Composition in Connection with Atmospheric New Particle Formation. Annual Review of Physical Chemistry, Vol 65 2014; 65: 21-37.
Kulmala M, Petaja T, Nieminen T, Sipila M, Manninen HE, Lehtipalo K, et al. Measurement of the nucleation of atmospheric aerosol particles. Nature Protocols 2012; 7: 1651-1667.
Lelieveld J, Evans JS, Fnais M, Giannadaki D, Pozzer A. The contribution of outdoor air pollution sources to premature mortality on a global scale. Nature 2015; 525: 367-371.
Liu J, Chu B, Chen T, Liu C, Wang L, Bao X, et al. Secondary Organic Aerosol Formation from Ambient Air at an Urban Site in Beijing: Effects of OH Exposure and Precursor Concentrations. Environmental Science & Technology 2018; 52: 6834-6841.
Liu JQ, Jiang JK, Zhang Q, Deng JG, Hao JM. A spectrometer for measuring particle size distributions in the range of 3 nm to 10 mu m. Frontiers of Environmental Science & Engineering 2016; 10: 63-72.
Liu XG, Li J, Qu Y, Han T, Hou L, Gu J, et al. Formation and evolution mechanism of regional haze: a case study in the megacity Beijing, China. Atmospheric Chemistry and Physics 2013; 13: 4501-4514.
Lu KD, Hofzumahaus A, Holland F, Bohn B, Brauers T, Fuchs H, et al. Missing OH source in a suburban environment near Beijing: observed and modelled OH and HO2 concentrations in summer 2006. Atmospheric Chemistry and Physics 2013; 13: 1057-1080.
Lu Y, Yan C, Fu Y, Chen Y, Liu Y, Yang G, et al. A proxy for atmospheric daytime gaseous sulfuric acid concentration in urban Beijing. Atmos. Chem. Phys. 2019; 19: 1971-1983.
Mao J, Ren X, Brune WH, Olson JR, Crawford JH, Fried A, et al. Airborne measurement of OH reactivity during INTEX-B. Atmospheric Chemistry and Physics 2009; 9: 163-173.
Mirme S, Mirme A. The mathematical principles and design of the NAIS - a spectrometer for the measurement of cluster ion and nanometer aerosol size distributions. Atmospheric Measurement Techniques 2013; 6: 1061-1071.
Molteni U, Bianchi F, Klein F, El Haddad I, Frege C, Rossi MJ, et al. Formation of highly oxygenated organic molecules from aromatic compounds. Atmospheric Chemistry and Physics 2018; 18: 1909-1921.
Parrish DD, Hahn CJ, Williams EJ, Norton RB, Fehsenfeld FC, Singh HB, et al. INDICATIONS OF PHOTOCHEMICAL HISTORIES OF PACIFIC AIR MASSES FROM MEASUREMENTS OF ATMOSPHERIC TRACE SPECIES AT POINT ARENA, CALIFORNIA. Journal of Geophysical Research-Atmospheres 1992; 97: 15883-15901.

394 Peng JF, Hu M, Wang ZB, Huang XF, Kumar P, Wu ZJ, et al. Submicron aerosols at thirteen diversified
395 sites in China: size distribution, new particle formation and corresponding contribution to cloud
396 condensation nuclei production. Atmospheric Chemistry and Physics 2014; 14: 10249-10265.
397 Petäjä T, Mauldin IRL, Kosciuch E, McGrath J, Nieminen T, Paasonen P, et al. Sulfuric acid and OH
398 concentrations in a boreal forest site. Atmos. Chem. Phys. 2009; 9: 7435-7448.
399 Shen XJ, Sun JY, Zhang XY, Zhang YM, Zhang L, Fan RX. Key features of new particle formation events
400 at background sites in China and their influence on cloud condensation nuclei. Frontiers of
401 Environmental Science & Engineering 2016; 10: 05.
402 Sun YL, Chen C, Zhang YJ, Xu WQ, Zhou LB, Cheng XL, et al. Rapid formation and evolution of an
403 extreme haze episode in Northern China during winter 2015. Scientific Reports 2016; 6: 27151.
404 Tan ZF, Rohrer F, Lu KD, Ma XF, Bohn B, Broch S, et al. Wintertime photochemistry in Beijing:
405 observations of ROx radical concentrations in the North China Plain during the BEST-ONE
406 campaign. Atmospheric Chemistry and Physics 2018; 18: 12391-12411.
407 Vanhanen J, Mikkila J, Lehtipalo K, Sipila M, Manninen HE, Siivola E, et al. Particle Size Magnifier for
408 Nano-CN Detection. Aerosol Science and Technology 2011; 45: 533-542.
409 Wang L, Wen L, Xu C, Chen J, Wang X, Yang L, et al. HONO and its potential source particulate nitrite
410 at an urban site in North China during the cold season. Science of The Total Environment 2015a;
411 538: 93-101.
412 Wang YH, Liu ZR, Zhang JK, Hu B, Ji DS, Yu YC, et al. Aerosol physicochemical properties and
413 implications for visibility during an intense haze episode during winter in Beijing. Atmospheric
414 Chemistry and Physics 2015b; 15: 3205-3215.
415 Yang F, Tan J, Zhao Q, Du Z, He K, Ma Y, et al. Characteristics of PM2.5 speciation in representative
416 megacities and across China. Atmospheric Chemistry and Physics 2011; 11: 5207-5219.
417 Yang YD, Shao M, Kessel S, Li Y, Lu KD, Lu SH, et al. How the OH reactivity affects the ozone
418 production efficiency: case studies in Beijing and Heshan, China. Atmospheric Chemistry and
419 Physics 2017; 17: 7127-7142.
420 Yao L, Garmash O, Bianchi F, Zheng J, Yan C, Kontkanen J, et al. Atmospheric new particle formation
421 from sulfuric acid and amines in a Chinese megacity. Science 2018; 361: 278-281.
422 Ye XN, Ma Z, Zhang JC, Du HH, Chen JM, Chen H, et al. Important role of ammonia on haze formation
423 in Shanghai. Environmental Research Letters 2011; 6: 024019.
424 Yuan B, Shao M, de Gouw J, Parrish DD, Lu SH, Wang M, et al. Volatile organic compounds (VOCs) in
425 urban air: How chemistry affects the interpretation of positive matrix factorization (PMF) analysis.
426 Journal of Geophysical Research-Atmospheres 2012; 117.
427 Zhao PS, Dong F, He D, Zhao XJ, Zhang XL, Zhang WZ, et al. Characteristics of concentrations and
428 chemical compositions for PM2.5 in the region of Beijing, Tianjin, and Hebei, China. Atmospheric
429 Chemistry and Physics 2013; 13: 4631-4644.
430 Zhou Y, Dada L, Liu Y, Fu Y, Kangasluoma J, Chan T, et al. Variation of size-segregated particle number
431 concentrations in wintertime Beijing. Atmos. Chem. Phys. 2020; 20: 1201-1216.
432 Zou Y, Deng XJ, Zhu D, Gong DC, Wang H, Li F, et al. Characteristics of 1 year of observational data of
433 VOCs, NOx and O-3 at a suburban site in Guangzhou, China. Atmospheric Chemistry and Physics
434 2015; 15: 6625-6636.
435